The Martian Zonal-Mean Circulation: Angular Momentum and Potential Vorticity Structure in GCM Simulations

JEFFREY R. BARNES

College of Oceanic and Atmospheric Sciences, Oregon State University, Corvallis, Oregon

ROBERT M. HABERLE

Space Sciences Division, NASA/Ames Research Center, Moffett Field, California

(Manuscript received 15 June 1995, in final form 6 June 1996)

ABSTRACT

Analysis of simulations performed with the NASA/Ames Mars GCM shows that under dusty conditions the Northern Hemisphere winter solstice circulation becomes characterized by a zonally averaged state in which the potential vorticity at upper levels is very small outside of high latitudes. The available observational data—in particular the 15-μm observations obtained by the Viking IRTM during the 1977 winter solstice global dust storm—provide evidence for changes in the Martian circulation that are basically like those found in the GCM. In the Mars GCM simulations for dusty solstice conditions, an extremely intense and approximately angular-momentum-conserving Hadley circulation is responsible for creating the low potential vorticity configuration. This can be contrasted with the Venus–Titan numerical simulations discussed by Allison et al. in which quasi-barotropic eddies appear to be largely responsible for the existence of low potential vorticity in lower and midlatitudes. At a near-equinox season the simulated Mars circulation is greatly weakened in comparison to that for solstice conditions, angular momentum is not approximately conserved by the mean meridional circulation, and potential vorticity increases relatively smoothly away from the equator.

1. Introduction

Allison et al. (1994) recently showed that numerical experiments intended to represent some aspects of the slowly rotating Venus–Titan circulation regimes were marked by an approximate approach toward a zero potential vorticity (ZPV) limit. In these simulations this appeared to be a result of the horizontal mixing of potential vorticity (PV) by quasi-barotropic eddies. In view of the constraints imposed by inertial instability on the PV distribution near the equator and the expectation that eddy instability and mixing processes might act to keep the gradients of PV relatively small, Allison et al. argued that a ZPV limit might tend to be approached by such a circulation. Assuming a latitudinally uniform Richardson number, Allison et al. obtained analytic expressions for the zonal wind and temperature fields corresponding to the ZPV limit and showed that the available Venus observational (wind) data are approximately consistent with these at three different atmospheric levels.

In this paper we present results from numerical experiments with the NASA/Ames Mars GCM that indicate that the simulated Martian zonal-mean circulation also tends toward a low PV state under certain conditions. For GCM experiments with significant atmospheric dust loadings, near northern winter solstice, the zonal-mean circulation at upper levels in the simulations is characterized by small PV values in lower and midlatitudes. The basic mechanism responsible for this is different from that in the Venus–Titan simulations since the mean meridional circulation becomes intense enough to approximately conserve angular momentum. As discussed by Allison et al. (1994), in the limit of large Richardson number, uniform absolute angular momentum and ZPV are equivalent, though for finite Richardson numbers this equivalence no longer holds. The upper-level, poleward-moving branch of the Hadley cell in the Mars GCM becomes approximately angular momentum conserving for dusty conditions near solstice (as the cell expands in both latitude and depth), and a low PV state is established throughout much of the lower- and midlatitude atmosphere. Farther poleward in the winter hemisphere, the PV jumps sharply to very large values that peak just poleward of the westerly jet core.

Observations obtained by the Viking IRTM instrument provide very good evidence that the kinds of changes in the zonal-mean circulation that occur in the Mars GCM with increasing dustiness near northern winter solstice also take place in the Martian atmo-

Corresponding author address: Dr. Jeffrey R. Barnes, College of Oceanic and Atmospheric Sciences, Oregon State University, Oceanography Administration Building 104, Corvallis, OR 97331-5503.

sphere. In particular, the 15-μm channel observations of a global dust storm event near northern winter solstice in 1977 are clearly consistent with a dramatic expansion and intensification of the cross-equatorial Hadley circulation (Martin and Kieffer 1979; Haberle et al. 1982; Zurek et al. 1992). The GCM simulations exhibit rather similar characteristics as the dust loading is increased, though at very high northern latitudes the model atmosphere is not warmed significantly (Zurek et al. 1992; Haberle et al. 1993).

For relatively nondusty conditions and near-equinox seasons the zonal-mean circulation in the Mars GCM is much weaker, angular momentum is not approximately conserved, and the zonal-mean PV increases relatively steadily away from the equator. The simulated Martian zonal-mean circulations thus span an extremely broad range as the strength of the thermal forcing increases, from relatively Earth-like circulations with weak zonal winds near equinox to the extremely unearthlike circulations obtained for dusty conditions at solstice. Mars presents itself as a natural laboratory for the investigation of the influence of thermal forcing on a rapidly rotating terrestrial-type atmosphere.

In the next section, we review some of the basic theory and modeling results that pertain to angular momentum and potential vorticity in zonally symmetric circulations and discuss the relevance of these to the Martian atmosphere. In the following section the structure of the angular momentum and potential vorticity fields in the GCM simulations is examined. Finally, we discuss and summarize the principal findings of this study.

2. Aspects of zonal-mean circulation: Theory and Mars

Held and Hou (1980) examined some of the basic aspects of nearly inviscid zonally symmetric circulations and showed that such a circulation will tend to produce a region of small potential vorticity as a result of the approximate conservation of angular momentum in the upper branch of the Hadley cell. In fact, symmetric instabilities associated with small negative values of PV (in the northern hemisphere) posed a direct difficulty to obtaining numerical solutions for steady circulations. For relatively weak thermal forcing (small thermal Rossby number), Held and Hou showed that the zonal wind and temperature fields corresponding to uniform angular momentum and ZPV would be approximately the same.

Allison et al. (1994) showed that uniform angular momentum corresponds to ZPV in the limit of infinite (and latitudinally uniform) Richardson number for a balanced zonal flow. The Held and Hou model is consistent with this since the difference between the symmetric wind and temperature fields corresponding to constant angular momentum and ZPV goes to zero as the Richardson number becomes large. Allison et al. argued that the ZPV limit might tend to be approached even for zonal-mean circulations that do not approximately conserve angular momentum as a result of PV mixing by eddies. They showed that numerical simulations intended to represent certain basic aspects of the Venus and Titan circulation regimes were in fact characterized by approximate ZPV. In these flows, the Richardson numbers are not large and ZPV does not correspond to uniform angular momentum. Allison et al. (1994) showed that the available observational zonal wind data for Venus at the cloud and ~25-km levels are largely consistent with ZPV for Richardson numbers of 2 and 1, respectively. At higher levels (~32 mb), the winds (as inferred from thermal data) are consistent with ZPV for large Richardson numbers.

The Held and Hou model for nearly inviscid circulations is of relevance for Mars because of the fact that the mean meridional circulation becomes sufficiently intense under dusty solstice conditions as to approach a state of angular momentum conservation in its upper branch. In particular, the ratio of a dynamical overturning timescale τ_D to a viscous dissipation timescale τ_v becomes relatively small because of the increasing strength of the thermal forcing. The smallness of this ratio is a key assumption underlying the Held and Hou nearly inviscid model. Assuming that the Richardson number remains large, then the fact that the upper portion of the Hadley cell is approximately angular momentum conserving implies that this region must be close to the ZPV limit. The zonally symmetric simulations of Haberle et al. (1982) clearly showed the tendency of the Martian solstice circulation to approach angular momentum conservation at upper levels as the atmospheric dust loading increased. Haberle et al. discussed the constraints on the latitudinal extent of the Hadley cell imposed by angular momentum conservation but did not examine the angular momentum and PV distributions in their simulations. They did note that symmetric instabilities presented problems in the absence of a Richardson number-dependent mixing scheme in their symmetric model.

Figure 1 shows the zonally averaged zonal wind and temperature fields from three experiments with the Ames Mars GCM: one for a near-equinox season and a small atmospheric dust loading (a visible optical depth of 0.3), a second for a period near northern winter solstice and a small dust loading (optical depth 0.3), and a third for the same solstice season and a large dust loading (an optical depth of 5). The atmospheric dust in the GCM simulations has a prescribed and static distribution, which corresponds to nearly uniform mixing throughout the lower portions of the atmosphere (see Pollack et al. 1990; Haberle et al. 1993). Haberle et al. (1993) examined a number of the Mars GCM simulations and characterized some of the basic features and properties of the zonal-mean circulation. In particular, they showed that the strength of the Hadley circulation in lower and midlatitudes varies dramatically with dust

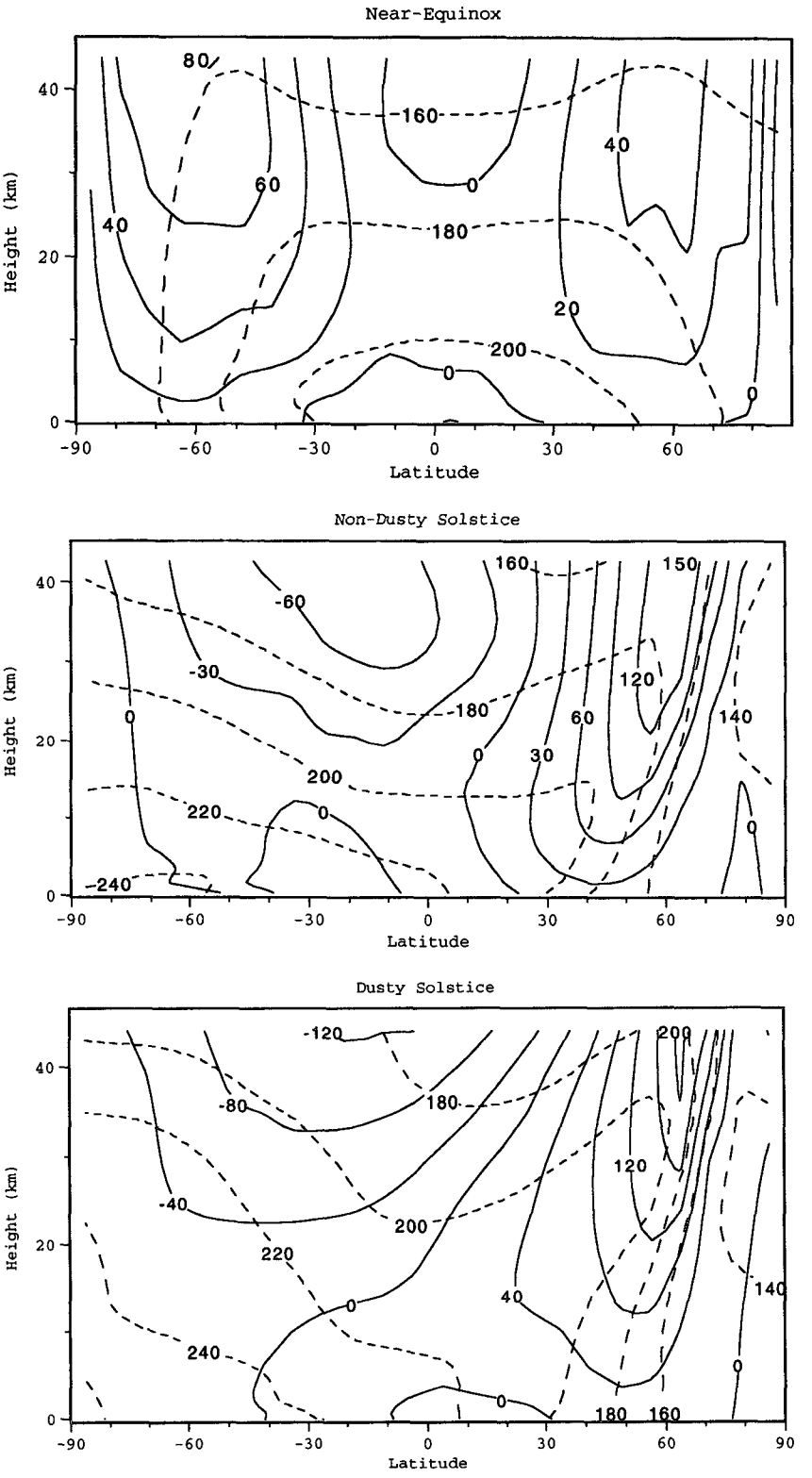

FIG. 1. Time and zonally averaged zonal winds (solid contours) and temperatures (dashed contours) from three GCM simulations: (a) near equinox with a low dust loading (optical depth 0.3), (b) northern winter solstice with a low dust loading (optical depth 0.3), and (c) northern winter solstice with a high dust loading (optical depth 5).

loading and season. The magnitude of the mass flow in the Hadley cell in the northern hemisphere varies by a factor of nearly 40 between the experiment for a very dusty (optical depth 5) northern winter solstice period and the relatively nondusty near-equinox (early northern spring) experiment (see Fig. 3). Corresponding to this, there is a tremendous change in the strength of the zonally averaged zonal winds, as illustrated in Fig. 2: the peak zonal wind speeds in the northern hemisphere in the near-equinox experiment are only about 40 m s^{-1}, whereas in the dusty solstice case the winds exceed 210 m s^{-1}. It is significant to note that the northern and southern Mars seasons are very asymmetric, largely because of the substantial eccentricity of Mars' orbit (hemispheric asymmetries in the topography also contribute substantially to this difference). In particular, GCM experiments for southern winter solstice yield a considerably weaker (by roughly a factor of 2) Hadley cell than those for northern winter solstice for given dust loadings. The peak zonal wind speeds in the southern winter solstice cases are somewhat weaker (by ~15%–25%) than those for northern winter solstice.

Figure 3 shows the mean overturning mass streamfunctions for the three GCM simulations in Fig. 1. The tremendous increase in both the strength and the extent of the Hadley circulation with changing season and increasing dust loading (increasing thermal forcing) is readily apparent.

It can be noted that the great increase in the strength of the zonal-mean circulation and large change in the atmospheric thermal structure that occur in the northern winter solstice simulations as the dust loading increases (see Haberle et al. 1993) are similar to behavior obtained in annual simulations with the recently developed French (LMD) Mars GCM (Hourdin et al. 1995). More importantly, though, these changes are essentially consistent with those observed by the Viking IRTM 15-μm channel during the 1977 winter solstice global dust storm (Martin and Kieffer 1979; Haberle et al. 1993). The Ames GCM does not produce a polar warming as was observed, but the temperature increases south of ~60°–70°N are similar to those seen in 1977. As discussed by Haberle et al., the GCM 15-μm temperatures are systematically colder than those observed, but this is due to the assumptions about the vertical and/or horizontal dust distributions and/or to assumptions about the infrared optical properties of the Mars dust. The zonally symmetric simulations of Haberle et al. (1982) actually produced overly warm temperatures in the 15-μm channel (at the ~25-km level) for large dust loadings. Haberle et al. (1993) also compared GCM simulations for a relatively nondusty season closer to equinox (somewhat later in northern spring than the near-equinox case examined here) with *Mariner 9* IRIS observations and showed that the general agreement was relatively good.

Table 1 summarizes some of the changes in the zonal-mean circulation in the three GCM simulations, giving the peak zonal wind speeds (in the Northern Hemisphere) along with estimates of a dynamical timescale (τ_D) for the Hadley circulation. The latter is simply based upon the mean meridional flow speed (a rough average in the upper branch of the Hadley cell)

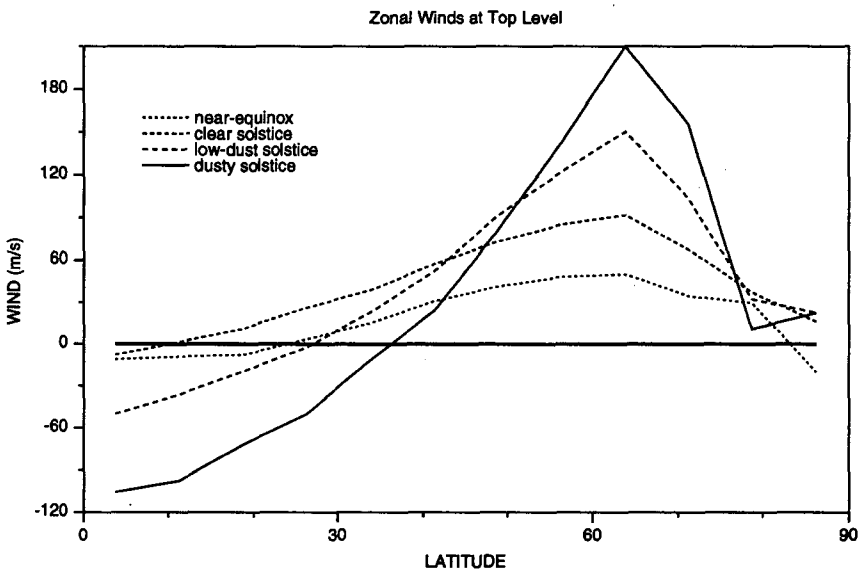

FIG. 2. Latitudinal profiles of the zonal-mean zonal wind at the top model level for the three GCM simulations in Fig. 1, along with the zonal wind from an additional northern winter solstice simulation without dust.

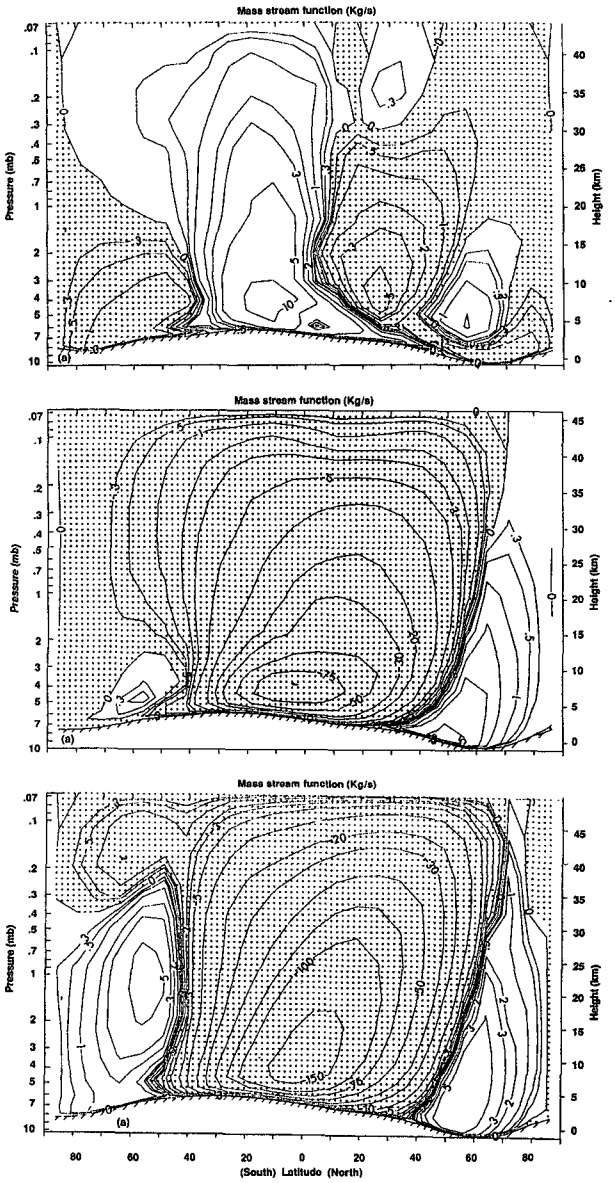

FIG. 3. Mean overturning mass streamfunction for the three GCM simulations in Fig. 1: (top) near equinox, (middle) nondusty solstice, and (bottom) dusty solstice. The units are 10^8 kg s^{-1}, and the circulation is clockwise around negative regions. Note that the contour intervals are not uniformly spaced.

and the planetary radius. Also shown in Table 1 are estimates of mechanical dissipation timescales (τ_v) and ratios of the dynamical to the dissipation timescales. The dissipation timescales are based upon eddy-mixing coefficient estimates for the GCM simulations (Barnes et al. 1996b). The peak zonal winds in Table 1 are also expressed in terms of an absolute angular momentum deficit (relative to the equator), and the values reflect the approach of the highly dusty solstice Mars circulation toward uniform momentum. The ratio of the dynamical to the dissipation timescale is of particular relevance in the context of the nearly inviscid theory of zonally symmetric circulations: this ratio must be small in order for the Hadley circulation to be approximately angular-momentum conserving (Held and Hou 1980). It can be seen from Table 1 that this ratio ranges from larger than unity in the relatively nondusty near-equinox case down to only ~0.1 in the dusty solstice case. Thus, the simulated Mars zonal-mean circulations span a very broad range, with an expectation that they not be angular momentum conserving at the one extreme but approach a nearly inviscid behavior at the other extreme.

Also shown in Table 1 are the corresponding parameter values for the earth's atmosphere, the troposphere, and the midatmosphere separately, as well as parameter estimates for the above-cloud atmosphere of Venus [the ~30-mb region; from Walterscheid et al. (1985)]. The latter may constitute a relatively inviscid zonal-mean circulation, as measured by the smallness of the momentum deficit in the core of the midlatitude jets (at ~50°–55° latitude) and the ratio of dynamical and dissipation timescales. The observational data seem to show that these jets fluctuate significantly in strength, however (Newman et al. 1984; Walterscheid et al. 1985). The earth mean circulations would not be expected to be particularly angular momentum conserving based upon the magnitudes of the dynamical–dissipation timescale ratio, but in terms of angular momentum deficit they can be considered to be as or more angular-momentum conserving (a latitude of 40° has been used for the earth's tropospheric jet, and for a latitude of 30° the angular momentum is substantially smaller) than the near-equinox and nondusty solstice Mars circulations. The latter have much greater latitudinal extents than their Earth counterparts, with the peak zonal winds being located at ~65°. At latitudes similar to those of the jets on earth (~40°), the Martian flows are as or more momentum-conserving than their terrestrial counterparts.

Figure 4 shows the distributions of the zonal-mean Richardson number in the three GCM experiments. It can be seen that at upper levels (above ~20 km) the Richardson number values are relatively large in the near-equinox and the relatively nondusty winter solstice simulations. However, in the dusty winter solstice case there is a region of relatively small Richardson numbers at upper levels, in lower latitudes, and extending into northern midlatitudes near the model top. Thus, in this case uniform angular momentum and ZPV profiles do not correspond to each other, even if gradient wind balance holds. It can be noted that the Richardson numbers would be even smaller in the dusty solstice simulation if they were computed using the total wind shear instead of just the zonal wind shear.

The mean zonal flow is well out of gradient wind balance at upper levels in lower and middle northern

TABLE 1. Mean circulation parameters.

	$\bar{u}$ (m s^{-1})	$(M_{EQ} - M)/M_{EQ}$	$\bar{v}$ (m s^{-1})	τ_D (days)	τ_v (days)	τ_D/τ_v
Mars equinox	~40	~0.7	~10.5	~80	~30	~3
Mars solstice	~150	~0.4	~8	~5	~20	~0.3
Mars dusty solstice	~210	~0	~40	~1	~10	~0.1
Earth troposphere	~35	~0.35	~1	~50	~10	~5
Earth middle atmosphere	~80	~0.28	~5	~10	~10	~1
Venus	~150	~0.15	~5–10?	~5–10?	~25?	~0.2–0.4?

latitudes in the dusty solstice simulation, however. This is evident in Fig. 1, where it can be seen that in this region there is strong easterly shear of the zonal flow but temperature decreases poleward (the minimum temperature at upper levels, outside of polar latitudes, is located at about 30°–35°N). The unbalanced state of the zonal winds is due to the extremely strong mean meridional flow in this region, with these winds peaking at over 80 m s^{-1} between ~30°–40°N. Advection of meridional momentum becomes a very important term in the (meridional) mean momentum balance in this region, in the dusty solstice simulation. In the nondusty solstice and near-equinox cases, the zonal flow remains close to gradient balance in this region since the meridional flow is much weaker than in the dusty solstice experiment.

One particular aspect of the current Mars GCM that is of relevance for the results discussed here is the presence of a Rayleigh friction sponge layer near the model top. The uppermost model layer has a frictional time constant of 2 days, with this increasing in the two layers below. Sensitivity experiments show that this friction layer acts to reduce the strength of the flow in the upper branch of the Hadley cell, but the effect upon the zonally averaged zonal wind and temperature fields is relatively small. The sponge layer acts generally to inhibit the angular momentum conserving nature of the circulation, making it less nearly inviscid (but it may at least crudely mimic some of the effects of breaking gravity waves and tides). The model top, corresponding to vanishing sigma vertical velocity, is located at a height of ~47 km in the current version of the Mars GCM. The most intense flows in the upper branch of the Hadley cell, in the simulations for dusty solstice conditions, occur at the highest model level.

3. Angular momentum and PV in the Mars GCM simulations

Figure 5 shows the zonally averaged absolute angular momentum fields, along with the potential temperature fields, for the three different Mars GCM simulations. The tendency of the Hadley circulation to "wrap up" the momentum contours as the rapidity of the overturning increases is apparent. In fact, in the very dusty solstice case the angular momentum field closely resembles the mass streamfunction field in lower and midlatitudes (see Fig. 3). In sharp contrast, the momentum field in the near-equinox experiment is only slightly modified from that for a motionless atmospheric state. The angular momentum field for a GCM solstice experiment with a "moderate" dust loading (an optical depth of 1, not shown) is quite similar to that for the very dusty case, while the solstice simulation with a low dust loading does not evidence as much wrapping up of the contours. The upper-level structure in the solstice cases reflects the considerable deepening of the Hadley circulation with increasing dustiness and a very intense northward meridional flow at high levels (see Haberle et al. 1993). This flow reaches ~80 m s^{-1} in the dusty solstice case and ~50 m s^{-1} in the moderate dust (unit optical depth) experiment; in the low dust (optical depth 0.3) solstice simulation the maximum meridional winds are not much in excess of 10 m s^{-1}, while in the near-equinox case the maximum meridional flow is only ~1–2 m s^{-1} at upper levels.

The potential temperature fields in Fig. 5 reflect the extent of the Hadley circulation in the extratropical atmosphere, as well as its intensity. The potential temperature field for the near-equinox simulation is relatively close to radiative equilibrium, particularly in the extratropical atmosphere. In contrast, the dynamical heating produced by the much stronger Hadley cells in the solstice cases is very apparent in the winter extratropical atmosphere, especially in the upper half of the model domain. In the highly dusty solstice case the upper-level temperature contours can be seen to be "wrapped up" in low and middle northern latitudes, with a very sharp transition to the higher-latitude temperature regime that is relatively unaffected by dynamical heating. The associated large horizontal gradients are in approximate thermal wind balance with the zonal jet, poleward of ~50°N. (As noted earlier, at lower latitudes gradient balance does not hold in the dusty solstice simulation because of the intense meridional jet.) The upper-level maximum in potential temperature between ~50°–60°N corresponds to the region of strongest sinking motion near the edge of the Hadley cell.

Figure 6 shows latitudinal profiles from the GCM simulations, at the highest model level (~45–50 km), of a measure of absolute angular momentum. The

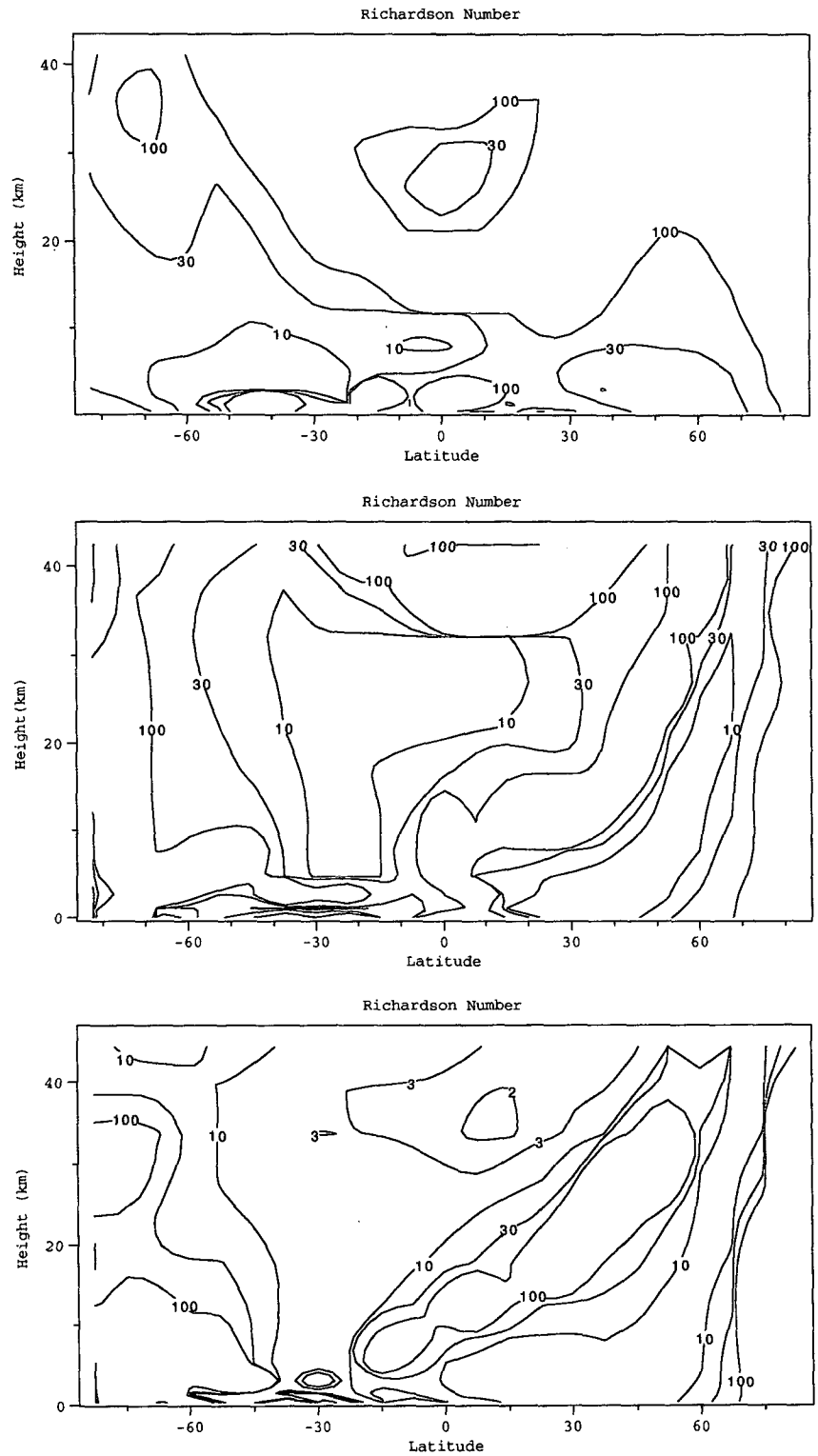

FIG. 4. Values of the Richardson number computed from the zonal-mean zonal wind and temperature fields in Fig. 1.

quantity that is plotted is the deficit in angular momentum relative to the value at the first GCM latitude in the northern hemisphere normalized by that value. The approach—as the mean meridional circulation becomes much more intense—of the simulated zonal flows to a state of approximately uniform angular momentum is evident in Fig. 6. At somewhat lower levels, the profiles of angular momentum are similar, especially in the near-equinox and nondusty solstice cases (see Fig. 5). In the dusty solstice simulation, the absolute angular momentum begins to decrease at significantly lower latitudes at lower levels, such that it decreases substantially in midlatitudes (see Fig. 5).

In Fig. 6, it can be noted that the angular momentum actually increases with increasing latitude in the dusty solstice case. This also occurs in very low latitudes in the nondusty solstice experiment. In low latitudes, equatorward of ~20°N, this could be due to the mean vertical advection of momentum, but at higher latitudes this cannot be the case as the vertical motion becomes downward. This aspect of the angular momentum distribution will be discussed below.

The wrapping up of the potential temperature and angular momentum contours in the dusty solstice simulation in low and midlatitudes, in the upper half of the model domain, results in the two approaching a parallel orientation. This implies that the zonal-mean PV is relatively small (see Allison et al. 1994) in this region, and this is indeed the case in the dusty solstice simulation. Figure 7 shows the mean PV fields, estimated according to (3) in Allison et al., for the three GCM simulations, and Fig. 8 illustrates the latitudinal PV profiles at the top model level (~47 km). In the near-equinox case, the PV values increase relatively smoothly away from the equator at all heights. In contrast, in the dusty solstice case the values at upper levels remain relatively small before increasing very rapidly in the extratropics at the edge of the Hadley cell. At high levels, the PV values equatorward of ~60°N are less than 10% of the maximum value (at that level) in polar latitudes. The values in the southern (summer) hemisphere are everywhere less than 10% of the northern polar maximum. At lower model levels, the PV increases to relatively larger values (compared to the high-latitude maximum at a given level) at lower latitudes: the PV maximum shifts strongly southward with decreasing height. This shift parallels, at somewhat higher latitudes, the northward tilt with height of the zonal jet (see Fig. 1). There are very large horizontal gradients in PV just equatorward of the maximum and similarly large negative gradients just poleward of it. The latter structure is associated with a sharp decrease in zonal wind speeds on the poleward side of the winter jet, as can be seen in Figs. 1 and 2.

The development of a much sharper jet structure, on the poleward side of the jet, with increasingly rapid overturning in the Hadley cell is something that is very evident in simple model simulations of zonally symmetric circulations (Held and Hou 1980). It was also apparent in the earlier zonally symmetric Martian simulations (Haberle et al. 1982). The Mars GCM employs a longitudinal smoothing at higher latitudes for numerical purposes, and this, along with the limited meridional resolution of the model (7.5°), may be acting to limit the sharpening of the jet somewhat in the simulations here. Of course, large-scale eddy processes could be playing a significant role in this also since the strongly negative PV gradients on the poleward flanks of the jet should be highly unstable.

At upper levels in lower and midlatitudes in the dusty solstice case, the Richardson numbers become fairly small (~2–3, see Fig. 4). Thus, a ZPV state does not correspond to a state of uniform angular momentum (Allison et al. 1994). Furthermore, gradient wind balance does not hold equatorward of ~30°–40°N in this simulation, such that the analytic expression obtained by Allison et al. for Ri = 2 is not appropriate either (even to the extent that the latitudinal variation of the Ri values can be neglected). Generally, an approximate ZPV state implies that

$$\frac{\partial M}{\partial \phi} \approx \left(\frac{\partial M}{\partial z} \frac{\partial \bar{\theta}}{\partial \phi} \right) \Big/ \frac{\partial \bar{\theta}}{\partial z},$$

where M is the absolute angular momentum and θ is the potential temperature. A negative meridional temperature gradient together with an easterly vertical shear of the zonal wind, as is present at upper levels in the dusty solstice case (and in the nondusty solstice case), thus implies an increase of angular momentum with latitude for approximate ZPV. As noted above, this is the case in the dusty solstice simulation at upper levels (see Fig. 6).

At lower latitudes and upper levels, the PV is significantly negative in the northern hemisphere in the dusty solstice simulation (see Figs. 7 and 8). The PV is closer to zero at low latitudes in the near-equinox simulation, with positive values to the north and negative values to the south of the equator. Advection of PV by the very strong northward meridional flow at high levels in the dusty solstice simulation is producing the region of negative values, which extends well into the winter hemisphere. The mean flow is therefore inertially unstable in this region—in the absence of dissipation—but manifestations of this instability are not present in the GCM zonal-mean wind fields (see Haberle et al. 1993). This could be due to the effect of dissipative processes or to the limited vertical resolution (about one-half scale height) of the Mars GCM. Eddy circulations that may be associated with inertial instability are present at lower latitudes in the northern winter solstice GCM simulations, as discussed by Barnes et al. (1993). These eddies, which seem to be "coupled" to the transient baroclinic eddies in middle and higher latitudes, may be acting to keep the PV val-

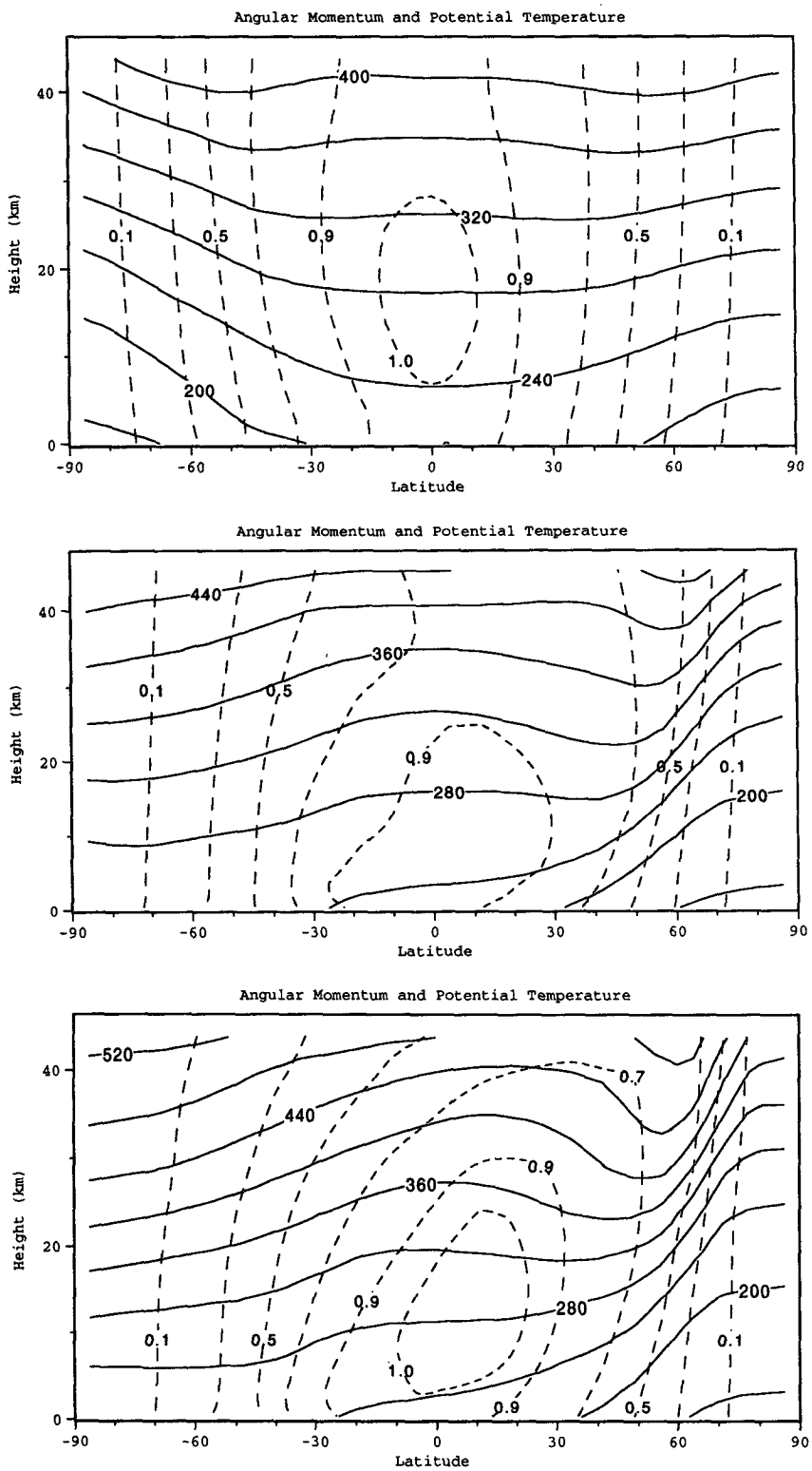

FIG. 5. Zonally and time-averaged absolute angular momentum (dashed contours, normalized by Ωa^2) and potential temperature (solid contours) for three Mars GCM simulations: (a) near equinox, (b) northern winter solstice with a low dust loading (optical depth 0.3), and (c) northern winter solstice with a high dust loading (an optical depth of 5).

ues closer to zero than they would be in the presence of only the zonal-mean circulation.

However, the transient eddies do not appear to be directly producing the increase of angular momentum with latitude that exists in the dusty solstice simulation. The pattern of Eliassen–Palm flux divergence in this case is such as to generally produce a decrease in angular momentum with latitude equatorward of 50°–60°N. However, the momentum tendency due to convective mixing in the GCM is such as to lead to an increase in angular momentum with latitude in the northern subtropical region at upper levels. The bulk of this convective mixing may be being triggered by large-scale eddies, including thermal tides and inertial instabilities. It thus appears as if eddies may be indirectly responsible for generating the increase in angular momentum with latitude that characterizes the dusty solstice simulation.

4. Discussion

Simulations with the NASA/Ames Mars GCM exhibit dramatic changes in the atmospheric structure with changes in the seasonal date and dust loading, as discussed by Haberle et al. (1993). We have examined the distributions of zonally averaged absolute angular momentum and PV in several of these simulations to further characterize the circulation changes. For northern winter solstice conditions, with substantial dust loadings, the upper-level atmosphere tends toward a state in which PV is very small outside of polar latitudes. This state bears some resemblence to the ZPV state discussed by Allison et al. (1994) as being of possible relevance for the Titan and Venus atmospheres. In the Martian numerical simulations, the low PV state is produced primarily by an approximately angular-momentum-conserving Hadley circulation and not by eddy mixing as in the slowly rotating simulations examined by Allison et al. The low PV configuration in the Mars GCM begins to be well defined in northern winter solstice simulations with relatively low dustiness (optical depths of 0.3) and then is greatly enhanced as the dust loading is further increased and the ratio of the dynamical timescale to the (mechanical) dissipation timescale becomes relatively small. In contrast to these cases, a near-equinox simulation with a low dust loading (and a relatively large ratio of dynamical to dissipative timescales) is characterized by a relatively smooth increase of PV and decrease of angular momentum away from the equator in lower and midlatitudes. The distribution of PV in this case is basically similar to that which exists in the middle and upper troposphere of the earth's atmosphere (Sun and Lindzen 1994).

Though the mean circulation clearly plays a dominant role in producing the zonally averaged state in the GCM simulations, it appears that large-scale eddies may be acting to keep the PV closer to zero in the northern subtropics and midlatitudes in the dusty solstice simulations. Zonally symmetric circulations resulting from inertial instability are not evident in the GCM simulations, though they were prominent in previous 2D numerical experiments in the absence of a Richardson number-dependent adjustment scheme. Convective mixing of momentum

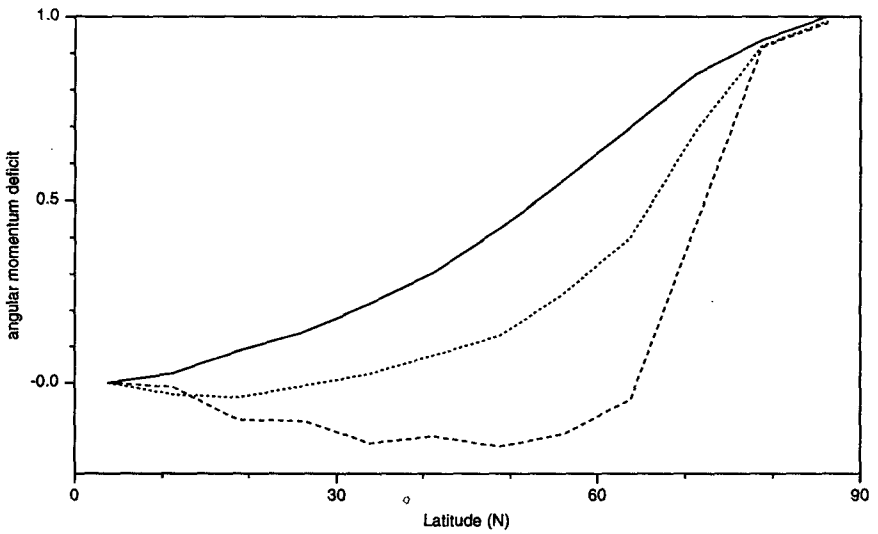

FIG. 6. Latitudinal profiles of a measure of the absolute angular momentum, $(M_{EQ} - M)/M_{EQ}$, at the highest model level, for the three Mars GCM experiments: near equinox (solid), northern winter solstice with a low dust loading (dotted), and northern winter solstice with a high dust loading (dashed). A value of zero corresponds to constant angular momentum in the northern hemisphere.

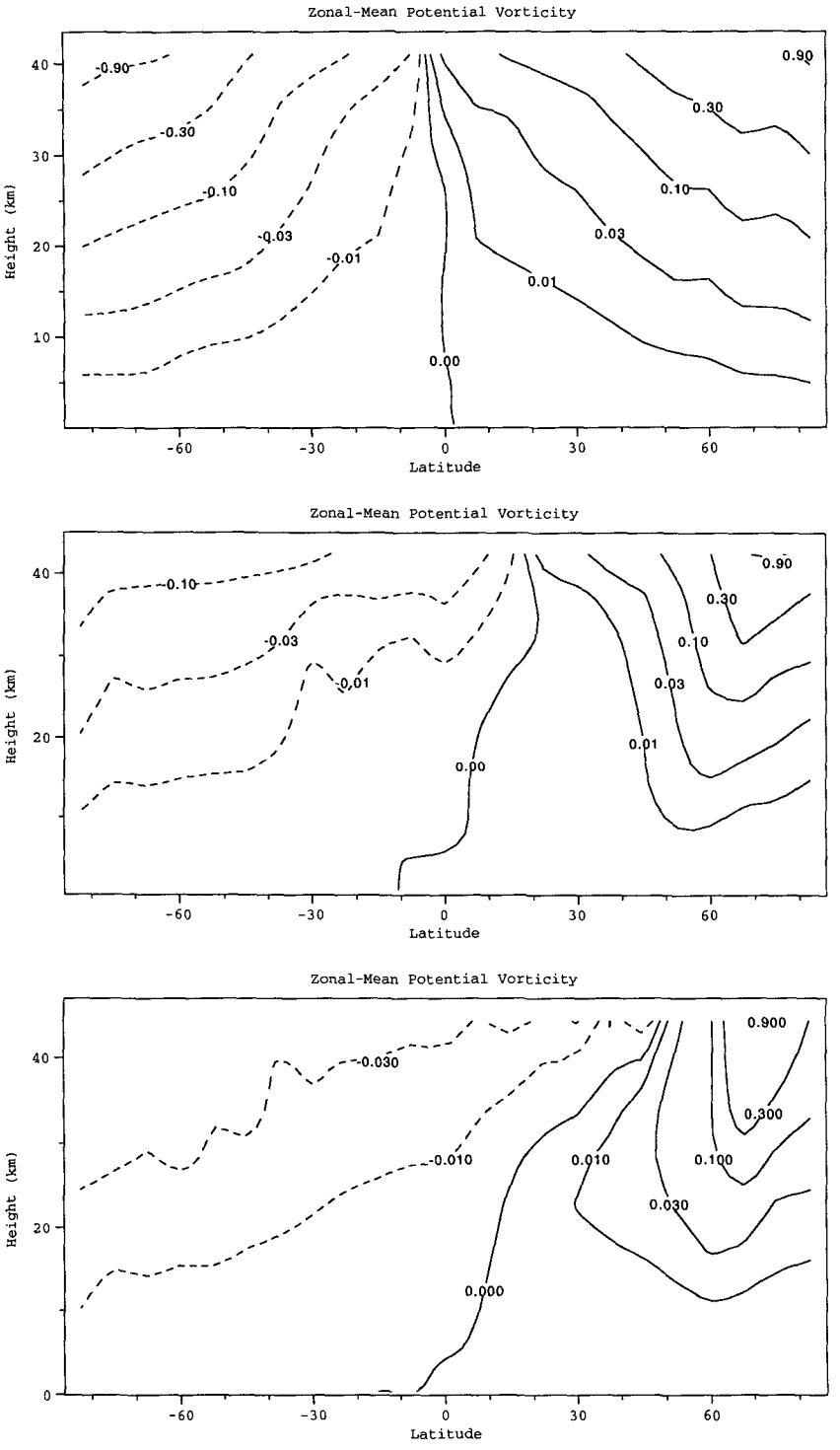

FIG. 7. Zonal-mean PV (calculated as in Allison et al. 1994) for the three Mars GCM experiments in Fig. 1. In each case values have been normalized by the maximum value in the field. Note that the contour levels are not linearly spaced but are approximately logarithmic.

triggered by large-scale eddies seems to be largely responsible for producing an increase of angular momentum with latitude at upper levels, corresponding to an approximate ZPV state in the presence of easterly zonal wind shear and poleward-decreasing temperatures.

Outside of the region of low PV in the solstice simulations there are very sharp gradients, both positive and negative, in polar latitudes. Analysis of the GCM data indicates that there are vigorous eddies (both transient and stationary) in this region, and these eddies exhibit maximum amplitudes in the region of large positive gradients, near the maximum in the PV (Barnes et al. 1993, 1996a). The existence of the very strong PV gradients (a large effective beta parameter) allows the eddies to penetrate vertically despite the extremely high zonal winds in the jet core, essentially according to the Charney–Drazin criterion (Barnes et al. 1996a). The eddy heat and momentum fluxes appear to be largely such as to mix PV horizontally (transport it downgradient) in this region. The eddies, though, are unable to reduce the PV gradients much in the presence of the extremely strong zonal-mean forcing. It can be noted that recent studies with a simplified Mars GCM have shown directly that eddy-induced changes to the zonal-mean flow are generally small (Haberle et al. 1996, manuscript submitted to *J. Geophys. Res.*). The transient polar warming observed by Viking during the winter solstice global dust storm in 1977 appears to be an example of much larger eddy-induced changes in the mean flow (Martin and Kieffer 1979; Jakosky and Martin 1987; Barnes and Hollingsworth 1987).

The variations in the structure of the zonal-mean circulation in the GCM simulations would seem to be basically consistent with theoretical expectations. In particular, the Hadley circulation becomes approximately angular momentum conserving when the thermal forcing becomes sufficiently strong that the ratio of a dynamical timescale to a mechanical dissipation timescale becomes relatively small (see Table 1). In this regime, as discussed above, it appears that the circulation is adjusting so as to stay near the ZPV limit. For the mean zonal wind and thermal structure at upper levels (which is not in gradient balance), this actually implies that there is a small but significant increase in angular momentum with latitude within the Hadley cell.

In the highly dusty solstice simulation, the zonal winds at upper levels bear some resemblence to those expected for a global angular momentum-conserving Hadley cell forced by a solstice heating field, with radiative equilibrium temperatures increasing monotonically toward the summer (south) pole (Schneider 1983). In particular, the summer easterlies peak at $\sim$130 m s^{-1} at $\sim$20°S, which can be compared with a wind of $\sim$190 m s^{-1} at this latitude for zero absolute angular momentum. In an experiment with a smaller dust loading (unit optical depth) but without a Rayleigh friction sponge layer, the easterly winds peak at $\sim$150 m s^{-1} at 20°S. Of course, vertical advection of angular momentum by the mean circulation is responsible for producing a very sharp increase in angular momentum in the GCM between $\sim$20°S and the equator.

An interesting aspect of the GCM results, in comparison to those obtained with simplified models (Schneider 1983), is that the temperature minimum at upper levels is not at the equator (see Fig. 1) but rather is located at $\sim$30°–45°N. The temperature distribution in lower and middle northern latitudes reflects the out

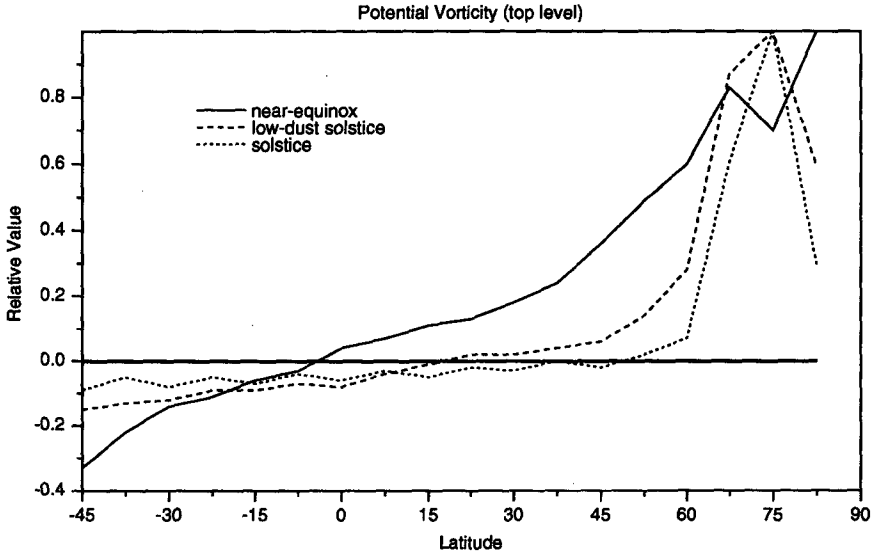

FIG. 8. Latitudinal profiles of zonal-mean PV at the top model level for the three GCM simulations in Fig. 6.

of gradient balance wind field, as discussed earlier. In the simplified models, the equatorial temperature minimum corresponds to gradient wind balance for the zero angular momentum state (Schneider 1983). In the GCM circulation, as noted above, vertical momentum advection causes the upper-level flow to deviate greatly from zero angular momentum in the tropics. The earlier zonally symmetric numerical simulations (Haberle et al. 1982) did produce a near-equatorial temperature minimum at upper levels, however, so the structure in the current GCM experiments may be due largely to eddy effects.

The available observational data are sparse and not adequate for the direct estimation of potential vorticity fields. However, the available temperature data can be compared with the GCM thermal fields. Haberle et al. (1993) discussed such comparisons and showed that fairly good agreement existed for a northern midspring seasonal date when the circumpolar jet is intensifying in the southern hemisphere and the northern jet is very weak (much as in the near-equinox case examined here). Conrath (1981) and Santee and Crisp (1993, 1995) presented *Mariner 9* IRIS observations for a late northern winter season, and Pollack et al. (1990) showed that the Mars GCM could produce similar zonal-mean thermal fields for this season. Barnes et al. (1996b) showed that there was also very good agreement in a timescale for "stratospheric" ventilation between that estimated by Santee and Crisp from the *Mariner 9* data and the Mars GCM. Unfortunately, there is not a suitable (possessing sufficient longitude coverage) dataset for a northern winter solstice seasonal date, but Viking 15-μm IRTM data for the ~25-km atmospheric level indicate that strong meridional temperature gradients are present in polar latitudes near solstice under dusty conditions (Martin and Kieffer 1979; Leovy 1982; Zurek et al. 1992). The temperature maximum that exists at these levels in middle to high latitudes in the observations is comparable (~210 K) to that produced in the highly dusty (optical depth 5) GCM northern winter solstice simulation; the somewhat colder GCM 15-μm temperatures are probably due mostly to assumptions about the vertical dust distribution and the dust optical properties (Haberle et al. 1993). The maximum in the IRTM observations is located somewhat poleward of that in the GCM, indicative of a broader Hadley circulation than exists in the model.

An important issue in connection with the results discussed here is to what extent they may be influenced by the location of the GCM top (at ~47 km). Experiments with a significantly higher top would be very much of interest, and several have recently been performed with the Mars GCM. These evidence only relatively slight changes in the structure of the zonal-mean flow below ~50 km. Various modeling studies have shown that gravity wave breaking could be a dominant process in the Martian middle atmosphere at altitudes above ~40–50 km (Barnes 1990; Joshi et al. 1995). Zonal jets as strong as those simulated by the current version of the Mars GCM may not exist in the presence of gravity wave processes. In this regard it can be noted that the Ames GCM has recently been run with a gravity wave parameterization, and the structure of the mean flow below ~50 km is not much different from that in the simulations examined here.

Acknowledgments. The lead author's work has been supported by a grant from the Planetary Atmospheres Program of NASA and by a Cooperative Agreement with the NASA/Ames Research Center. The Mars GCM project at Ames has been supported by the Planetary Atmospheres Program of NASA. The efforts and leadership of the late James B. Pollack were both instrumental and inspirational in the development and utilization of the Mars GCM as a unique atmospheric modeling tool. This study would not have been possible without his contributions.

REFERENCES

Allison, M., A. D. Del Genio, and W. Zhou, 1994: Zero potential vorticity envelopes for the zonal-mean velocity of the Venus/Titan atmospheres. *J. Atmos. Sci.*, **51,** 694–702.

Barnes, J. R., 1990: Possible effects of breaking gravity waves on the circulation of the middle atmosphere of Mars. *J. Geophys. Res.*, **95,** 1401–1421.

——, and J. L. Hollingsworth, 1987: Dynamical modeling of a planetary wave mechanism for a Martian polar warming. *Icarus,* **71,** 313–334.

——, J. B. Pollack, R. M. Haberle, C. B. Leovy, R. W. Zurek, H. Lee, and J. Schaeffer, 1993: Mars atmospheric dynamics as simulated by the NASA Ames General Circulation Model, 2. Transient baroclinic eddies. *J. Geophys. Res.*, **98,** 3125–3148.

——, R. M. Haberle, J. B. Pollack, H. Lee, and J. Schaeffer, 1996a: Mars atmospheric dynamics as simulated by the NASA Ames General Circulation Model, 3. Winter quasi-stationary eddies. *J. Geophys. Res.*, **101,** 12 753–12 776.

——, T. D. Walsh, and J. R. Murphy, 1996b: Transport time scales in the Martian atmosphere: GCM simulations. *J. Geophys. Res.*, **101,** 16 881–16 889.

Conrath, B. J., 1981: Planetary-scale wave structure in the Martian atmosphere. *Icarus,* **48,** 246–255.

Haberle, R. M., C. B. Leovy, and J. B. Pollack, 1982: Some effects of global dust storms on the atmospheric circulation of Mars. *Icarus,* **50,** 322–367.

——, J. B. Pollack, J. R. Barnes, R. W. Zurek, C. B. Leovy, J. Murphy, H. Lee, and J. Schaeffer, 1993: Mars atmospheric dynamics as simulated by the NASA Ames General Circulation Model, 1. The zonal-mean circulation. *J. Geophys. Res.*, **98,** 3093–3123.

——, H. Houben, J. R. Barnes, and R. Young, 1996: A simplified 3D model for Mars climate studies. *J. Geophys. Res.*, in press.

Held, I. M., and A. Y. Hou, 1980: Nonlinear axially symmetric circulations in a nearly inviscid atmosphere. *J. Atmos. Sci.*, **37,** 515–533.

Hourdin, F., F. Forget, and O. Talagrand, 1995: The sensitivity of the Martian surface pressure and atmospheric mass budget to various parameters: A comparison between numerical simulations and Viking observations. *J. Geophys. Res.*, **100,** 5501–5523.

Jakosky, B. M., and T. Z. Martin, 1987: Mars: North polar atmospheric temperatures during dust storms. *Icarus,* **72,** 528–534.

Joshi, M. M., B. N. Lawrence, and S. R. Lewis, 1995: Gravity wave drag in 3D atmospheric models of Mars. *J. Geophys. Res.*, **100,** 21 235–21 245.

Leovy, C. B., 1982: Martian meteorological variability. *Adv. Space Res.*, **2,** 19–44.

Martin, T. Z., and H. H. Kieffer, 1979: Thermal infrared properties of the Martian atmosphere, 2. The 15-μm band measurements. *J. Geophys. Res.*, **84,** 2843–2852.

Newman, M., G. Schubert, A. J. Kliore, and I. R. Patel, 1984: Zonal winds in the middle atmosphere of Venus from Pioneer Venus radio occultation data. *J. Atmos. Sci.*, **41,** 1901–1913.

Pollack, J. B., R. M. Haberle, J. Schaeffer, and H. Lee, 1990: Simulations of the general circulation of the Martian atmosphere I. Polar processes. *J. Geophys. Res.*, **95,** 1447–1474.

Santee, M., and D. Crisp, 1993: Thermal structure and dust loading of the Martian atmosphere during late southern summer: Mariner 9 revisited. *J. Geophys. Res.*, **98,** 3093–3123.

——, and ——, 1995: Diagnostic calculations of the circulation in the Martian atmosphere. *J. Geophys. Res.*, **100,** 5465–5484.

Schneider, E. K., 1983: Martian great dust storms: Interpretative axially symmetric models. *Icarus,* **55,** 302–331.

Sun, D., and R. S. Lindzen, 1994: A PV view of the zonal mean distribution of temperature and wind in the extratropical troposphere. *J. Atmos. Sci.*, **51,** 757–772.

Walterscheid, R. L., G. Schubert, M. Newman, and A. J. Kliore, 1985: Zonal winds and the angular momentum balance of Venus' atmosphere within and above the clouds. *J. Atmos. Sci.*, **42,** 1982–1990.

Zurek, R. W., J. R. Barnes, R. M. Haberle, J. B. Pollack, J. E. Tillman, and C. B. Leovy, 1992: Dynamics of the atmosphere of Mars. *Mars*, H. H. Kieffer, B. M. Jakosky, C. W. Snyder, and M. Matthews, Eds., The University of Arizona Press, 835–933.